

New Finite-Difference Schemes for Constrained Non-Linear Parabolic Equations with Application to the Porous Medium Flows

Stanislav S Makhanov

Department of Information Technology, Sirindhorn International Institute of Technology,
Thammasat University, Rangsit Center, Patum Thani 12121, Thailand.
Corresponding author, E-mail: makhanov@siit.tu.ac.th

Received 27 Apr 2000

Accepted 8 Dec 2000

ABSTRACT We present a new family of numerical methods to solve non-linear parabolic initial boundary value problems with constraints imposed a priori on the solution. Firstly, we introduce our recent results developed for the diffusion wave equation endowed with one constraint (non-negativity of the solution). The numerical procedures are based on a consistent first-order approximation of diffusion and transport terms combined with the Gauss-Seidel-type iterative technique. Secondly, we show that the Richard's type models of porous medium flows exemplify the general case of a non-linear parabolic equation endowed with the bilateral constraints specified by characteristics of the porous medium. Therefore, we generalize the preceding numerical procedures to the Richard's type models of unsaturated flows in the soil. The Gauss-Seidel-type iterative technique is supplemented by a three-step numerical procedure employing auxiliary variables. We prove the convergence theorems and introduce some further extensions of the algorithm. Finally, we verify the proposed schemes by methodological applications and analyze the convergence rate.

KEYWORDS: finite-difference schemes, overland flow, porous medium, non-linear degenerate parabolic equation.

INTRODUCTION

We present a new family of numerical methods designed to solve numerically non-linear degenerate parabolic initial boundary-value problems endowed with constraints imposed a priori on the solution. The corresponding partial derivative equations are often employed in Environmental Fluid Dynamics to simulate open flows in the frame-work of shallow water theory^{1,3,5,6,7,9,10,11,15,23-26,28,30,33,35,36,39-41,43,44} as well as unsaturated porous medium flows in the frame work of Richard's equations.^{1,3,6,8,10,11,14,16-20,23,24,29,33,36,38,39}

There exists a number of well-established classical methods to solve numerically the parabolic systems³⁷ as well as versatile techniques designed to treat degenerate parabolic equations.^{2,13,21,22,32} However, to the best of our knowledge the problem of a start-to-finish technique to treat degenerate parabolic equations endowed with constraints imposed a priori on the solution has received too little attention in the Literature.

A typical example is the conventional numerical treatment of the diffusion wave version of the shallow water equations. A physically relevant numerical

solution must satisfy $h \geq 0$ (where h is the water depth). However, the numerical schemes require a sophisticated control of possible non-negative components of the finite-difference solution in the regions characterized by a small water depth. Otherwise, any negative component of the numerical solution, appearing in the regions where h is near or equal to zero, generates undecaying oscillations (which do not allow any physical interpretation) and numerical instability. The current methods to suppress the instabilities are quite heuristic having been mainly reduced to some particular regularization.^{5,6,11,32} Moreover, none of the conventional finite-difference or finite-elements techniques guarantees non-negativity of the flow depth without a special kind of smoothing, artificial correction, forced refinement of the grid or a special numerical treatment based the boundary tracking methods (the so called wet-dry cell policies).^{6,25} Besides, the schemes based on finite elements often involve the so-called lumping regularization techniques⁹ which could substantially decrease the order of approximation.

Richard's equation of the unsaturated porous flows represents an initial boundary value problem for the non-linear parabolic equation endowed with

bilateral constraints specified by characteristics of the porous medium. As it is the case of the diffusion wave equation, the numerical treatment of the Richard's type equations requires a sophisticated control of possible violations of the prescribed bounds.

Our new numerical algorithms entirely eliminate the above mentioned drawbacks. We guarantee reliable calculations for a variety of water dynamics in the porous medium when the soil moisture approaches the prescribed bounds.

NUMERICAL ALGORITHMS FOR THE DIFFUSION WAVE EQUATION

In this section we present our previous numerical methods designed to numerically solve the non-linear degenerate diffusion wave equation. We present some theoretical results illustrated by new methodological applications.

The diffusion wave approach is often employed to simulate the overland flows, the flooding waves, flows in the open canals, estuaries, reservoirs as well as flows in the coastal zones. The diffusion wave equation is then derived in the frame-works of the shallow water theory⁴³ by assuming that the inertia forces are negligible.

In this case, the momentum equation is given by

$$\mathbf{grad}(\eta) + \frac{Q|Q|}{\alpha(h)} = 0.$$

The first term combines the pressure and the gravity force whereas the second term represents the friction force. $\mathbf{grad} \equiv (\partial/\partial x, \partial/\partial y)$, x, y are the spatial (horizontal) coordinates, $\eta \equiv \eta(x, y, t)$ denotes the free surface level, t the time coordinate. $\eta = h + z$, where $h \equiv h(x, y, t)$ is the flow depth and $z \equiv z(x, y)$ the bottom level. $Q \equiv Q(x, y, t)$ denotes the discharge vector and $\alpha \equiv \alpha(h)$ a semi-empirical function which characterizes the friction.

Substituting the corresponding components of the discharge vector into the continuity equation yields the diffusion wave equation given by

$$w_h \frac{\partial \eta}{\partial t} = \text{div}(\text{sign}(\alpha) \sqrt{|\alpha|} \mathbf{grad} \eta) + T,$$

where $T \equiv T(x, y, t, h)$ denotes the source (sink) and $w_h \equiv w_h(x, y, h)$ a coefficient related to the cross-sectional area of the flow.

Furthermore, $D \equiv D(h) = \text{sign}(\alpha) \sqrt{|\alpha|}$ is interpreted as the diffusion coefficient. In the case of one

dimensional open flows, $D = wR^{2/3} / (n_f |\frac{\partial \eta}{\partial x}|^{1/2})$,

$w_h \equiv w/h$, where $w = w(x, h)$ denotes the cross-sectional area of the flow, $R = R(x, h)$ the hydraulic radius⁸ and $n_f \equiv n_f(x, y)$ is the Manning coefficient characterizing roughness of the river or canal surface.

The two dimensional case implies $w_h \equiv 1$,

$$D = \frac{h^{5/3}}{n_f |\mathbf{grad} \eta|^{1/2}}.$$

Note that although we only involve the hydrodynamic interpretation of the equations, our theoretical results are valid for non-linear parabolic equations satisfying $D(x, y, 0) = 0$, $D/h < +\infty$, $|T/h| < +\infty$, if $T \leq 0$. In what follows we shall always assume (if not stated otherwise) that the above conditions hold.

Consider a one dimensional version of the equation. An obvious substitution $\eta = h + z$ yields

$$w_h \frac{\partial \eta}{\partial t} = D \frac{\partial^2 h}{\partial x^2} + \frac{\partial D}{\partial h} \frac{\partial h}{\partial x} \frac{\partial z}{\partial x} + D \frac{\partial^2 z}{\partial x^2} + T,$$

Note, that the third term constitutes a supplementary source(sink) which could produce negative values of the flow depth. Furthermore, if h is close or equal to zero the diffusion term $D(h)$ degenerates. However, although $h \rightarrow 0$ implies,

$D \frac{\partial^2 h}{\partial x^2} \rightarrow 0$, $\frac{\partial D}{\partial h} \frac{\partial h}{\partial x} \frac{\partial z}{\partial x}$ may not be vanishing.

Therefore, the degenerate diffusion coefficient invokes "hyperbolic" properties of the equation. A numerical scheme which does not "recognize" this phenomenon typically generates negative values of h leading to numerical instability. Fig 1 and Fig 2 illustrate instability of the conventional (unconditionally stable for the linear case !) fully implicit symmetric scheme employed to solve numerically a problem of overflow. The water flow is characterized by the linear friction $D = \chi h$, $\chi = 10^{-3} \text{ m}^2/\text{s}$. $0 \leq x \leq 1000$, $w = 100 \text{ m}$, the time step $\tau = 20 \text{ min}$, the space step $\Delta h = 15 \text{ m}$. The boundary conditions are given by $Q(0, t) = 10 \text{ m}^3/\text{s}$, $Q(1000, t) = 0$. The calculations clearly demonstrate that even small violations of the positivity of the water depth (Fig 1) induce unwanted oscillations and instability (Fig 2). Observe that the instabilities display the well-established phenomenon of a finite velocity of the disturbance propagation for non-linear parabolic equations first espoused by Barenblatt and Vishik.⁴ As a matter of fact, further analysis of non-linear degenerate parabolic systems shows that under certain conditions the equations generate breaking of waves and the shock waves.¹³

It should be noted, that there is an intuitive understanding of the impact of non-linearity of the de-generate diffusion wave equation in the hydrological literature as well. For instance,³⁸ proposes the so-called generalized flux law given by $Q = -a_1 h^m - a_2 \text{grad}(h)$, where a_1 , a_2 and m are the empirical constants. However, such a representation may not be always accurate since the transport term is actually *induced by non-linearity* of the equation. Consequently, there is no need for the proposed additional term $-a_1 h^m$.

Finally, an efficient numerical scheme must combine properties of the conventional procedures for parabolic equations with properties of the absolutely stable schemes for hyperbolic equations characterized by the Courant-Frederich-Levy-type (CFL) condition.

The key idea of such an algorithm for the one-dimensional case is based on the consistent first-order approximation of the hyperbolic (transport) terms by directed differences combined with the corresponding right-hand (left-hand) approximations for the diffusion terms and the Gauss-Seidel-iterations.²⁶

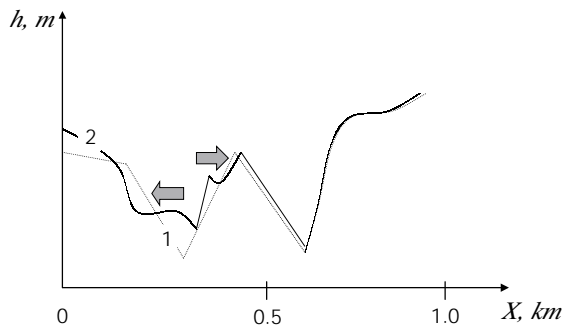


Fig 1. Numerical solution of the overflow problem. Development of instability for the conventional scheme, 10 iterations. (1) the ground level, (2) the water level ◼ the negative flow depth

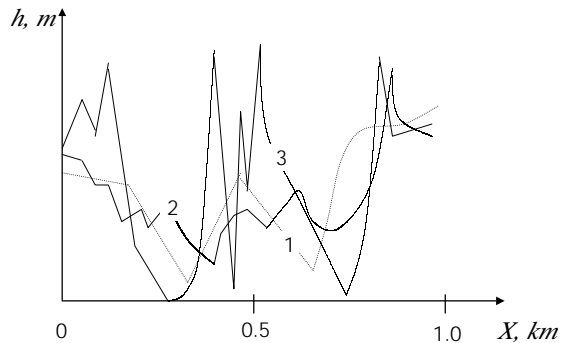


Fig 2. Overflow problem. Development of instability for the conventional scheme, (1) the ground level, (2) the water level, 30 iterations, (3) 40 iterations.

First, we represent the transport term by $\partial(hd)/\partial x$, where the identity $d=D/h$ always holds for small h (in so far that $D/h \rightarrow 0$ as $h \rightarrow 0$). Secondly, we approximate the transport term by directed differences in accordance with the hyperbolic properties of the diffusion wave equation. Thirdly, we use an implicit approximation of the diffusion term employing the corresponding right-hand(left-hand) grid points for $(dh)_k$.

Algorithm 1

$$(w_h)_k^{n+1} (\tilde{h}_k^{n+1} - h_k) / \tau = \{ \tilde{d}_{k+\alpha}^n [\tilde{h}_{k+\alpha}^n (\tilde{h}_{k+1}^{n+1} - \tilde{h}_k^{n+1}) + \tilde{h}_{k+\alpha,1}^{n+1} (z_{k+1} - z_k)] - \tilde{d}_{k-1+\beta}^n [\tilde{h}_{k-1+\beta}^n (\tilde{h}_k^{n+1} - \tilde{h}_{k-1}^{n+1}) + \tilde{h}_{k-1+\beta}^{n+1} (z_k - z_{k-1})] \} / \Delta x^2 + \tilde{T}_k,$$

n denotes the iteration number, symbol \sim the upper time layer, k the number of a grid point

$$a = a(k) = \begin{cases} 0, & \text{if } z_{k+1} - z_k \leq 0, \\ 1, & \text{otherwise,} \end{cases} \quad \beta = \beta(k) = \begin{cases} 0, & \text{if } z_k - z_{k-1} \leq 0, \\ 1, & \text{otherwise.} \end{cases}$$

The source term is approximated by means of the following regularization

$$\tilde{T}_k = \begin{cases} \tilde{T}_k^{n+1}, & \text{if } \tilde{T}_k^{n+1} > 0, \\ \frac{\tilde{T}_k^n \tilde{h}_k^{n+1}}{\tilde{h}_k^n}, & \text{otherwise.} \end{cases}$$

Theorem 1 The numerical solution \tilde{h}_k is non-negative.²⁶ Fig 3. displays a numerical solution to the overflow problem produced by the proposed scheme. The time and the space steps are identical to those employed by the conventional scheme (Fig 1-2). Clearly, the method establishes convergence and generates an oscillation-free numerical solution.

A two-dimensional version of the scheme is a

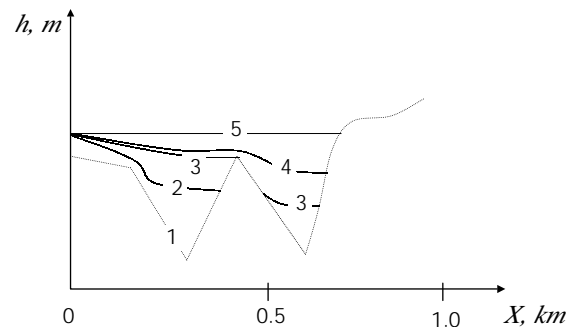


Fig 3. Overflow problem. (1)-the ground level, (2) the water level, 80 min, (3) -250 min, (4)-330 min, (5)-3000 min.

sum of the one- dimensional non-negative schemes with regard to the x and y direction.

Algorithm 2

$$\begin{aligned}
 (\tilde{h}_{k,l}^{n+1} - h_{k,l}) / \tau = & \{ \tilde{d}_{k+\alpha,l}^n [\tilde{h}_{k+\alpha,l}^n (\tilde{h}_{k+1,l}^{n+1} - \tilde{h}_{k,l}^{n+1}) + \\
 & \tilde{h}_{k+\alpha,l}^{n+1} (z_{k+1,l} - z_{k,l})] - \tilde{d}_{k-1+\beta,l}^n [\tilde{h}_{k-1+\beta,l}^n (\tilde{h}_{k,l}^{n+1} - \tilde{h}_{k-1,l}^{n+1}) + \\
 & \tilde{h}_{k-1+\beta,l}^{n+1} (z_{k,l} - z_{k-1,l})] \} / \Delta x^2 + \{ \tilde{d}_{k,l+\gamma}^n [\tilde{h}_{k,l+\gamma}^n (\tilde{h}_{k,l+1}^{n+1} - \tilde{h}_{k,l}^{n+1}) + \\
 & \tilde{h}_{k,l+\gamma}^{n+1} (z_{k,l+1} - z_{k,l})] - \tilde{d}_{k,l-1+\delta}^n [\tilde{h}_{k,l-1+\delta}^n (\tilde{h}_{k,l}^{n+1} - \tilde{h}_{k,l-1}^{n+1}) + \\
 & \tilde{h}_{k,l-1+\delta}^{n+1} (z_{k,l} - z_{k,l-1})] \} / \Delta y^2 + \hat{T}_{k,l},
 \end{aligned}$$

where

$$\begin{aligned}
 a \equiv a(k,l) = & \begin{cases} 0, & \text{if } z_{k+1,l} - z_{k,l} \leq 0, \\ 1, & \text{otherwise,} \end{cases} & \beta \equiv \beta(k,l) = & \begin{cases} 0, & \text{if } z_{k,l} - z_{k-1,l} \leq 0, \\ 1, & \text{otherwise,} \end{cases} \\
 \gamma \equiv \gamma(k,l) = & \begin{cases} 0, & \text{if } z_{k,l+1} - z_{k,l} \leq 0, \\ 1, & \text{otherwise,} \end{cases} & \delta \equiv \delta(k,l) = & \begin{cases} 0, & \text{if } z_{k,l} - z_{k,l-1} \leq 0, \\ 1, & \text{otherwise} \end{cases}
 \end{aligned}$$

and \hat{T}_k is an approximation analogous to that introduced in the 1D case.

Theorem 2 The numerical solution $\tilde{h}_{k,l}$ is non-negative.²⁷

Theorem 3 Algorithm 2 converges.²⁹

A large series of methodological 1D and 2D open flow modeling^{28, 30} as well as modeling of the flood in the Eastern Areas of Bangkok^{28, 30} has shown advantages the proposed method. Fig. 4-5 illustrate the typical test. The simulated 2D wave enters the region, propagates inside it and leaves across a section of the boundary. The flow is characterized by non-linear friction, $n_f=0.02 \text{ m}^{-1/3}/\text{s}$. Fig. 4 displays the ground elevations whereas Fig. 5 shows the depth of the open flow for $t=4$ and 10 h.

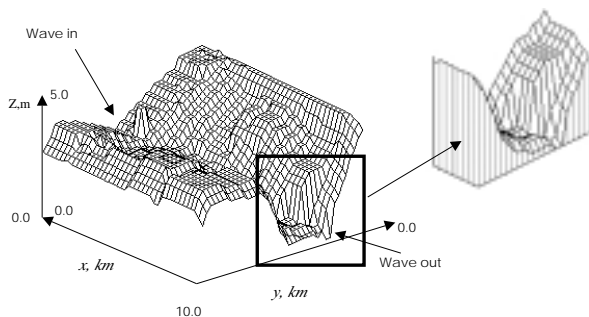


Fig 4. Surface wave propagation. Ground elevations.

Table 1 reveals an overall priority of the proposed scheme with regard to conventional methods. S_1 denotes the average number of iterations required by the proposed method, S_2 the number of iterations required by the standard three point, second order implicit scheme, S_τ the number of the time steps required by the fully explicit, second order scheme, $\Delta=\Delta x=\Delta y$, symbol (-) indicates presence of negative components, shadowed cells in the table specify the most suitable schemes.

Finally, we analyze the convergence rate. The error is estimated by $\|h - h_f\|_C$, $\|h - h_f\|_{L_1}$ and, $\|h - h_f\|_{L_2}$ where h_f is the solution obtained by the conventional scheme on a fine grid. The numerical experiments reveal that the convergence rate varies between $\Delta^{0.81}$ and $\Delta^{1.22}$ irrespectively of the norm.

Table 1. Efficiency of the algorithm. 2D surface wave.

S_1	S_2	S_τ	τ , sec	Δ , m
11	7(-)	7	10000	500
21	Diverges	34	50000	500
22	Diverges	67	100000	500
23	Diverges	334	500000	500
14	12(-)	14	10000	250
25	Diverges	67	50000	250
21	Diverges	134	100000	250
27	Diverges	667	500000	250
20	Diverges	27	10000	125
21	Diverges	134	50000	125
26	Diverges	267	100000	125
30	Diverges	1335	500000	125

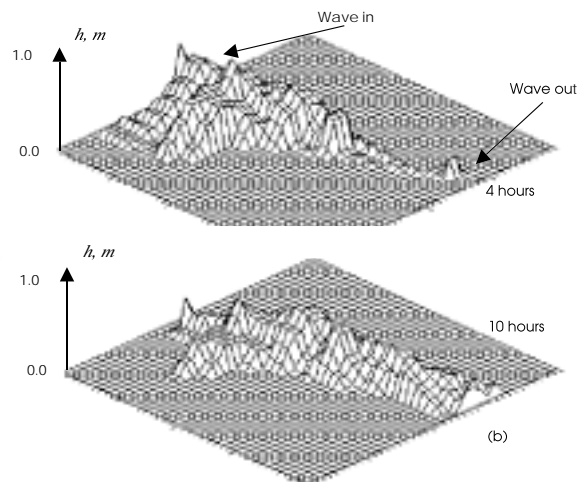


Fig 5. Surface wave propagation, $t=4$ and 10h.

RICHARD'S EQUATION

In this section we generalize our numerical procedures to the Richard's type models to simulate unsaturated porous medium flows.

Introduce a control volume of the porous medium ΔV . The volume of water in ΔW being measured by the moisture content is defined by $\theta \equiv \Delta W / \Delta V$. The porosity of the medium is defined by $\theta_{max} \equiv \Delta P / \Delta V$, where ΔP is the volume of voids. If the moisture content is equal to the porosity we shall call the porous medium saturated. Finally, the residual moisture content is defined by $\theta_{min} \equiv \Delta R / \Delta V$, where ΔR is a volume of water remaining in the porous medium after it has been thoroughly drained.

Furthermore, the theory of porous medium flows assumes that θ , θ_{max} and θ_{min} are piecewise continuous functions defined for $\forall x, y, z, t$. This approach to model porous medium flows has been extensively applied in groundwater hydrology to simulate saturated and unsaturated flows in the soil.^{1, 3, 6, 7, 8, 10, 11, 14, 16-20, 23, 24, 29, 33, 36, 38, 39}

The case of saturated flow through the soil implies that the momentum equation is represented by Darcy's Law

$$Q = -K \text{grad}(\eta),$$

where Q denotes the discharge, $K \equiv K(x, y, h)$ the hydraulic conductivity of the medium, η the free surface level and h the depth of the flow.

However, the *unsaturated* flows may not allow formulation in terms of a free-boundary problem. Consequently, η is thought of as the energy per unit weight of the fluid⁸ where a part of the total energy is referred as the capillary potential (the suction head) ψ . The total energy is then composed of the gravity and the capillary forces, $\eta = \psi - z$, where z is the vertical coordinate being positive downwards from an arbitrary datum within the soil column. Consequently, $Q = -K \text{grad}(\eta) = -K[\text{grad}(\psi) - (0, 0, 1)]$. Consider the one dimensional case. A 1D vertical

flow implies $Q = -K(\frac{\partial \psi}{\partial z} - 1)$.

Substituting Q into the continuity equation yields

$$\frac{\partial \theta}{\partial t} = \frac{\partial}{\partial z} K \frac{\partial \psi}{\partial z} - \frac{\partial K}{\partial z} + T,$$

where $T = T(\theta, t)$ denotes the source(sink).

There exists a number of well-established parametric models of the soil hydraulic functions $K \equiv K(\theta, z)$ and $\psi \equiv \psi(\theta, z)$. The largest group is based on the Brooks and Corey type formulas^{7, 8, 14} given by

$$\psi \equiv \psi(s, z) = \psi_1 s^{-1/p}, K \equiv K(s, z) = K_1 s^c, c \equiv c(z) = (2+3p)/p,$$

where $K_1 \equiv K_1(z)$, $\psi_1 \equiv \psi_1(z)$, $p \equiv p(z)$ depend on the type of soil (for instance, for clay $K_1 = 3.4 \cdot 10^{-5} \text{ cm s}^{-1}$, $\psi_1 = 90 \text{ cm}$ and $p = 0.44$ whereas for sand $K_1 = 8.6 \cdot 10^{-3} \text{ cm s}^{-1}$, $\psi_1 = 15 \text{ cm}$ and $p = 5.4$). The parameterizations are given in terms of a new variable $s = (\theta - \theta_{min}) / (\theta_{max} - \theta_{min})$ called the effective saturation. Typical graphs of the soil hydraulic functions are shown in Fig. 6-7. Finally note, that $\psi(1) = \psi_1 \neq 0$ only in the sense of the best empirical fit to the data. The theoretical value of ψ at $s=1$ ($\theta = \theta_{max}$) is zero.⁸

An equally popular Genuchten's parameterization^{18, 19} is given by

$$\Psi \equiv \Psi(s, z) = \Psi_1 (s^{\frac{p}{1-p}} - 1)^{1/p}$$

Clearly, $\Psi(1) = 0$. However, the first derivative of Genuchten's type functions is infinite at $s=1$. This feature presents some difficulties in constructing an appropriate approximation of Richard's equation with regard to θ . However, only the θ -version of Richard's equation allows an efficient control of the inequality $\theta_{min} \leq \theta \leq \theta_{max}$.

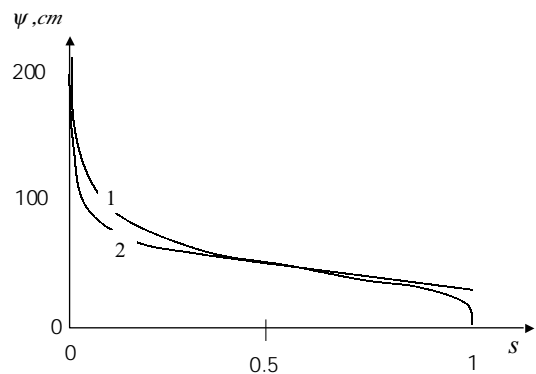


Fig 6. Parametric models of the capillary potential (1) the Brooks-Corey model, (2) Genuchten's model.

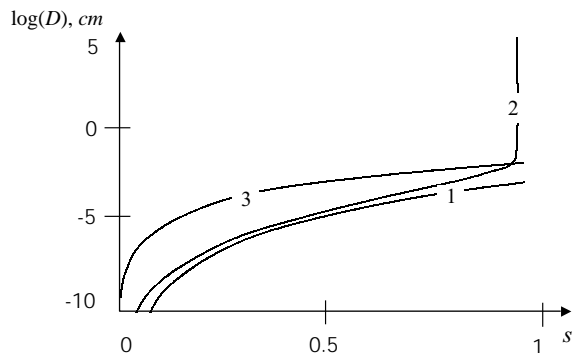


Fig 7. Typical soil hydraulic functions. (1) $\log(D(s))$ -Brooks-Corey model, (2) $\log(D(s))$ -Genuchten's model, (3)- $\log(K(ss))$

We derive the θ -version by writing $\frac{\partial \psi}{\partial z} = \Phi \frac{\partial \theta}{\partial z}$,

where $\Phi = \frac{\partial \psi}{\partial \theta} = \frac{\partial \psi}{\partial s} \frac{\partial s}{\partial \theta}$ and defining the soil water diffusivity by $D = K\Phi$. Substituting into Richard's equation yields

$$\frac{\partial \theta}{\partial t} = \frac{\partial}{\partial z} D \frac{\partial \theta}{\partial z} - \frac{\partial K}{\partial z} + T.$$

It is easy to verify that, in the case of the Brooks-Corey model $D = \psi_1 K_1 \frac{s^{1/p+2}}{p}$. Therefore $D(0) < \infty$, moreover, $D/s \rightarrow 0, D/s^2 \rightarrow 0$ as $s \rightarrow 0, \forall p > 1$ although $\psi(0) = \infty$ if $p > 1$.

Finally, the soil moisture content must not only satisfy Richard's equation but the inequality $\theta_{\min} \leq \theta \leq \theta_{\max}$ as well. Therefore, a problem of the unsaturated porous medium flow constitutes an initial boundary value problem for a non linear degenerate parabolic equation endowed with bilateral constraints.²⁹

A numerical treatment of such a boundary-value problem requires a sophisticated control of possible violations of the inequality. Otherwise, the numerical scheme typically generates undecaying oscillations and numerical instability near $\theta = \theta_{\min}$ or $\theta = \theta_{\max}$. Development of such instability is displayed in Fig 8-9. The figures demonstrate the numerical solution of an infiltration problem (propagation of water from the soil surface). Richard's equation is approximated by the conventional fully implicit symmetric iterative scheme. $0 \leq z \leq 200$ cm, $z=0$ corresponds to the soil surface, the time step $\tau=3$ min, the spatial step $\Delta z=5$ cm. The boundary conditions are given by $\theta(0,t)=\theta_{\max}(0)=0.5, \theta(200,t)=0.3$ where $\theta_{\max}, \theta_{\min}$ are the piecewise linear functions depicted in Fig 9.

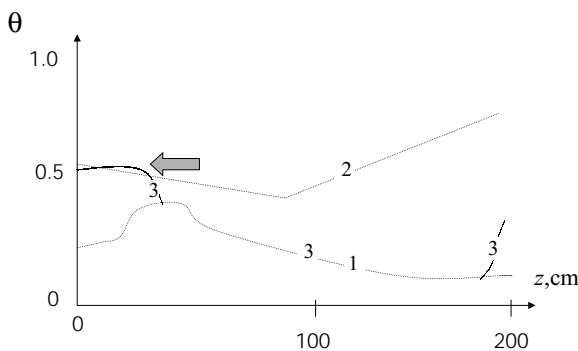


Fig 8. Numerical solution of Richard's equation. Development of instability for a conventional scheme, 5 iterations (1)- θ_{\min} , (2)- θ_{\max} , (3)- θ , \blackleftarrow -points where the constraints are violated.

The calculations clearly demonstrate that even small violations of the prescribed bounds (Fig. 8) could lead to the catastrophic oscillations shown in Fig. 9.

In order to construct a stable procedure which guarantees the prescribed constraints, we generalize the numerical algorithms proposed in the preceding chapters.

First, we consider the case $\theta_{\max} = \text{const}, \theta_{\min} = \text{const}$. Moreover, in what follows we shall always assume that $|T/(\theta - \theta_{\min})| < \infty$, if $T \leq 0, |T/(\theta_{\max} - \theta)| < \infty$ if $T > 0$.

Algorithm 2

Step 1 is based on the following representation $K = (\theta - \theta_{\min})^a = \mu a$. $a = a(\theta) = [K(\theta) - K(\theta_{\min})] / (\theta - \theta_{\min})$.

Clearly, $a(\theta_{\min}) < \infty$ since $K(\theta_{\min}) = 0$ and $\frac{\partial K}{\partial \theta}$ is bounded.

Next, we introduce an auxiliary variable $\mu = \theta - \theta_{\min}$ and apply Algorithm 2 to Richard's equation represented in terms of μ .

$$\begin{aligned} (\tilde{\mu}_m^{n+1} - \mu_m) / \tau &= [K_m^n \Phi_{m+1/2}^n (\tilde{\mu}_{m+1}^{n+1} - \tilde{\mu}_m^{n+1}) - \\ & (K_{m-1}^n \Phi_{m-1/2}^n (\tilde{\mu}_m^{n+1} - \tilde{\mu}_{m-1}^{n+1}))] / \Delta z^2 - \\ & (a_m^n \tilde{\mu}_m^{n+1} - a_{m-1}^n \tilde{\mu}_{m-1}^{n+1}) / \Delta z + \hat{T}_m^v, \end{aligned}$$

where

$$\hat{T}_m^v = \begin{cases} \tilde{T}_m^{n+1}, & \text{if } \tilde{T}_m^{n+1} > 0, \\ \frac{\tilde{T}_k^n \tilde{\mu}_m^{n+1}}{\tilde{\mu}_m^n}, & \text{otherwise.} \end{cases}$$

Note that, $\hat{T}_m^v = [\tilde{T}_m^{n+1}]^+ + [\tilde{T}_k^n]^- \tilde{\mu}_m^{n+1} / \tilde{\mu}_m^n$,

where $[f]^+ = 0.5(f + |f|), [f]^- = 0.5(f - |f|)$

Step 2 represents Richard's equation in terms of the second auxiliary variable $v = \theta_{\max} - \theta$.

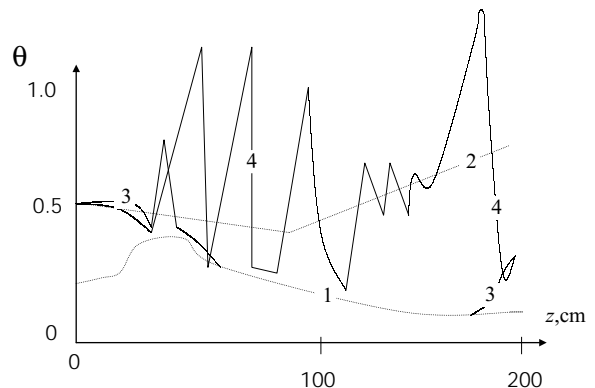


Fig 9. Numerical solution of Richard's equation. Development of instabilities for a conventional scheme, (1)- θ_{\min} , (2)- θ_{\max} , (3)- θ , 10 iterations, (4) - θ , 15 iterations.

It may seem that the new variable does not allow the required “diffusion-transport” form. However, since $K(\theta_{\max}) = K_1 = \text{const}$

$\frac{\partial K}{\partial z} = -\frac{\partial}{\partial z} [K(\theta_{\max}) - K(\theta)] = -\frac{\partial}{\partial z} (bv)$, where $b = b(\theta, z) = [K(\theta_{\max}, z) - K(\theta, z)] / (\theta_{\max} - \theta)$, $b(\theta_{\min}) = \infty$. A straightforward application of Algorithm 2 yields

$$(\tilde{v}_m^{n+1} - v_m) / \tau = [K_m^n \Phi_{m+1/2}^n (\tilde{v}_{m+1}^{n+1} - \tilde{v}_m^{n+1}) - K_{m-1}^n \Phi_{m-1/2}^n (\tilde{v}_m^{n+1} - \tilde{v}_{m-1}^{n+1})] / \Delta z^2 - (b_m^n \tilde{v}_m^{n+1} - b_{m-1}^n \tilde{v}_{m-1}^{n+1}) / \Delta z - \hat{T}_m^\mu,$$

where \hat{T}_m^μ is a regularization analogous to that introduced at step 1.

Finally, we perform the following correction

procedure $\tilde{\theta}_m^{n+1} = (\theta_{\min})_m + \frac{(\theta_{\max})_m - (\theta_{\min})_m}{\tilde{v}_m^{n+1} + \tilde{\mu}_m^{n+1}} \mu_m$, $m=1, \dots, N-1$.

Note, that step 3 guarantees the identity $\mu + v \equiv \theta_{\max} - \theta_{\min}$ which otherwise does not hold at the discrete level.

Furthermore, we prove basic properties of Algorithm 3.

Theorem 4 *The numerical solution satisfies*

$$\theta_{\min} \leq \tilde{\theta}_m^{n+1} \leq \theta_{\max}.$$

Proof. It is sufficient to establish $\mu \geq 0$ and $v \geq 0$. We shall only prove that $\mu \geq 0$. A proof of the inequality $v \geq 0$ is identical and therefore omitted.

Consider the first stage of the algorithm. Suppose that although at the previous time step $\mu_m \geq 0, \forall m$, after $n+1$ iterations the procedure generates negative components located at the interval $[m_1, m_2]$. In other words, $\tilde{\mu}_m^{n+1} < 0, m = m_1, \dots, m_2$

Summation of the finite-difference equations over $m = m_1, \dots, m_2$ yields

$$\sum_{m=m_1}^{m=m_2} \tilde{\mu}_m^{n+1} = \sum_{m=m_1}^{m=m_2} \mu_m^n + \tau [K_{m_2}^n \Phi_{m_2+1/2}^n (\tilde{\mu}_{m_2+1}^{n+1} - \tilde{\mu}_{m_2}^{n+1}) - K_{m_1-1}^n \Phi_{m_1-1/2}^n (\tilde{\mu}_{m_1}^{n+1} - \tilde{\mu}_{m_1-1}^{n+1})] / \Delta z^2 - \tau (a_{m_2}^n \tilde{\mu}_{m_2}^{n+1} - a_{m_1-1}^n \tilde{\mu}_{m_1-1}^{n+1}) / \Delta z + \sum_{m=m_1}^{i=m_2} \hat{T}_m^{n+1}$$

After some technical manipulations we have

$$\sum_{m=m_1}^{m=m_2} \tilde{\mu}_m^{n+1} (1 - \tau [\hat{T}_m^{n+1} / \mu_m^n]^-) - \tau (K_{m_2}^n \Phi_{m_2+1/2}^n / \Delta z + a_{m_2}^n) \tilde{\mu}_{m_2}^{n+1} / \Delta z - \tau K_{m_1-1}^n \Phi_{m_1-1/2}^n \tilde{\mu}_{m_1-1}^{n+1} / \Delta z^2 = \sum_{m=m_1}^{m=m_2} \tilde{\mu}_m^n + \tau \sum_{m=m_1}^{m=m_2} [\hat{T}_m^{n+1}]^+ + \tau K_{m_2}^n \Phi_{m_2+1/2}^n \tilde{\mu}_{m_2+1}^{n+1} / \Delta z^2 +$$

$$\tau (K_{m_1-1}^n \Phi_{m_1-1/2}^n / \Delta z + a_{m_1-1}^n) \tilde{\mu}_{m_1-1}^{n+1} / \Delta z.$$

Clearly, the left hand side is non positive.

Therefore, either or both $\tilde{\mu}_{m_1-1}^{n+1}$ and $\tilde{\mu}_{m_2+1}^{n+1}$ are not positive. Consequently the interval $[m_1, m_2]$ can be expanded to $[m_1-1, m_2]$ or to $[m_1, m_2+1]$ or to $[m_1-1, m_2+1]$. Continuing the same argument $\tilde{\mu}_m^{n+1} \leq 0, m=0, \dots, N$ yields. However, the statement is in contradiction with apparently non-negative $\tilde{\mu}_0^{n+1}, \tilde{\mu}_N^{n+1}$. Therefore $\tilde{\mu}_m^{n+1} \leq 0, \forall m$.

Remark Clearly, if $T \equiv 0$ then $\tilde{\mu}_m^{n+1} \equiv 0 \Leftrightarrow \tilde{\mu}_0^{n+1} = \tilde{\mu}_N^{n+1} = 0$.

The scheme is a discrete analogy of the mass conservation law.

This property can be easily verified by a straightforward summation over the computational domain.

Theorem 5 *Let a, b satisfy the Lipschitz-type conditions given by*

$$|[a(\theta_1) - a(\theta_2)] / (\theta_1 - \theta_2)| \leq A < \infty, |[b(\theta_1) - b(\theta_2)] / (\theta_1 - \theta_2)| \leq B < \theta_\infty,$$

$\forall \theta_1, \theta_2, \theta_1 - \theta_2 \neq 0$. where A, B are some constants, then Algorithm 3 converges.

Consider step 1. Let. $\sigma_m^{n+1} = \tilde{\mu}_m^{n+1} - \tilde{\mu}_m^n$. Obvious technical manipulations yield

$$\sigma_m^{n+1} = \tau [K_m^n \Phi_{m+1/2}^n (\sigma_{m+1}^{n+1} - \sigma_m^{n+1}) - K_{m-1}^n \Phi_{m-1/2}^n (\sigma_m^{n+1} - \sigma_{m-1}^{n+1})] / \Delta z^2 - (b_m^n \sigma_m^{n+1} - b_{m-1}^n \sigma_{m-1}^{n+1}) / \Delta z + \Delta_m^n,$$

where $\|\Delta_m^n\|_C \leq [2 \|\tilde{\mu}^n\|_C \|\Phi^n\|_C (\|a^n\|_C + \|\tilde{\mu}^{n-1}\|_C A) / \Delta z + \|\tilde{\mu}^n\|_C A] 2\tau \|\tilde{\sigma}^n\|_C / \Delta z$. It is easy to verify that coefficients of the 3-diagonal form of the system given by $A_{k,l} \sigma_{k-1,l}^{n+1} - C_{k,l} \sigma_{k,l}^{n+1} + B_{k,l} \sigma_{k+1,l}^{n+1} = -F_{k,l}^n$ satisfy $A_{k,l} > 0, B_{k,l} > 0, D_{k,l} = C_{k,l} - A_{k,l} - B_{k,l} > 0$.

Therefore, by theorem 3³⁷, page. 47. $\|\sigma^{n+1}\|_C \leq \|F^n\|_C$ Consequently, there exist such q_1, q_2 that $\|\sigma^{n+1}\|_C \leq \|\Delta^n\|_C < q_1 \|\sigma^{n+1}\|_C + q_2$, where q_1, q_2 can be made small enough by choosing an appropriate τ . It is also plain that, an analogous estimate can be derived with regard to $(\tilde{v}_m^{n+1} - v_m^n)$. Therefore, the method converges.

Remark. Observe that coefficients a and b corresponding to the Brooks and Corey model satisfy the conditions of Theorem 5.

Next, consider a porous medium with z-dependent characteristics, i.e. $\theta_{\min} = \theta_{\min}(z), \theta_{\max} = \theta_{\max}(z), K_1 = K_1(z)$, etc. Note, that in this case Richard's

equation no longer satisfies the maximum principle. For instance, the boundary conditions $\theta(0, t) = \theta(200, t) = \text{const}$ do not necessarily lead to the steady-state solution $\theta(z, t) = \text{const}$ (Fig. 10).

Algorithm 4

Consider step 1. A change of variables $\mu = \theta - \theta_{\min}$ yields $K = \mu a_1, a_1(\theta_{\min}) < \infty, \frac{\partial}{\partial z} D \frac{\partial \theta}{\partial z} - \frac{\partial K}{\partial z} = \frac{\partial}{\partial z} K \Phi \frac{\partial \mu}{\partial z} + \frac{\partial}{\partial z} (K \Phi \frac{d\theta_{\min}}{dz}) - \frac{\partial}{\partial z} (a_1 \mu) = \frac{\partial}{\partial z} K \Phi \frac{\partial \mu}{\partial z} + \frac{\partial}{\partial z} (a_1 a_2),$ where $a_2 = \mu (\Phi \frac{d\theta_{\min}}{dz} - 1).$

An approximation corresponding to the first step is then given by

$$(\bar{\mu}_m^{n+1} - \mu_m) / \tau = K_{m+\alpha}^n \Phi_{m+1/2}^n (\bar{\mu}_{m+1}^{n+1} - \bar{\mu}_m^{n+1}) / \Delta z^2 + (a_1)_{m+\alpha} (a_2)_{m+1/2}^n \bar{\mu}_{m+\alpha}^{n+1} / \Delta z - K_{m-1+\beta}^n \Phi_{m-1/2}^n (\bar{\mu}_m^{n+1} - \bar{\mu}_{m-1}^{n+1}) / \Delta z^2 - (a_1)_{m-1+\beta} (a_2)_{m-1/2}^n \bar{\mu}_{m-1+\beta}^{n+1} / \Delta z + \hat{T}_m^\mu,$$

where

$$(a_2)_{m+1/2}^n = \Phi_{m+1/2}^n (\frac{d\theta_{\min}}{dz})_{m+1/2} - 1, (\frac{d\theta_{\min}}{dz})_{m+1/2} = [(\theta_{\min})_{m+1} - (\theta_{\min})_m] / \Delta z, \alpha = \alpha(m) = \begin{cases} 0, & \text{if } (a_2)_{m+1/2}^n \leq 0, \\ 1, & \text{otherwise,} \end{cases} \beta = \beta(m) = \begin{cases} 0, & \text{if } (a_2)_{m-1/2}^n \leq 0, \\ 1, & \text{otherwise.} \end{cases}$$

Unfortunately, $\theta_{\max} = \theta_{\max}(z)$ does not allow a complete “diffusion-transport” form.

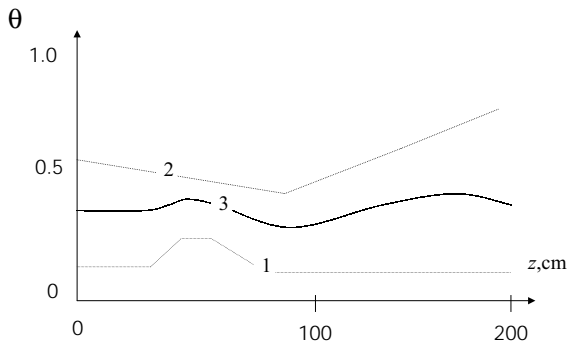


Fig 10. Violation of the maximum principle. (1)- θ_{\min} , (2)- θ_{\max} , (3) the steady-state solution corresponding to the boundary conditions $\theta(0, t) = 0.35, \theta(200, t) = 0.35.$

Therefore, we represent $\frac{\partial K}{\partial z}$ by

$$\frac{\partial K}{\partial z} = - \frac{\partial}{\partial z} [K(\theta_{\max}(z), z) - K(\theta, z)] + \frac{\partial K(\theta_{\max}(z), z)}{\partial z} = - \frac{\partial}{\partial z} (b_1 v) + \frac{dK_1}{d\theta_{\max}} \frac{d\theta_{\max}}{dz}, b_1(\theta_{\max}) < \infty.$$

Next, consider the diffusion term $D \equiv K \Phi$, where $\Phi = \frac{\partial \psi}{\partial \theta}$. Note, that neither the Brooks and Corey nor the Genuchten’s type functions satisfy $\frac{\partial \psi(s, z)}{\partial s} = 0$ at $s=1$. Therefore, we “repair” $\psi(s)$ at the interval $[1-\epsilon, 1]$ by means of the following regularization.

$$\psi^* \equiv \psi^*(s, z) = \begin{cases} \psi(s, z), & \text{if } s \leq 1 - \epsilon, \\ \varphi(s, z), & \text{otherwise,} \end{cases}$$

where $\varphi(s, z)$ is a Hermite polynomial satisfying $\varphi(1 - \epsilon, z) = \psi_\epsilon, \psi_\epsilon \equiv \psi_\epsilon(z) = \psi(1 - \epsilon, z),$

$$\frac{\partial \varphi(1 - \epsilon, z)}{\partial s} = \psi'_\epsilon, \psi'_\epsilon \equiv \psi'_\epsilon(z) = \frac{\partial \psi(1 - \epsilon, z)}{\partial s},$$

$$\varphi(1, z) = \psi(1, z), \frac{\partial \varphi(1, z)}{\partial s} = 0.$$

(See Fig. 11, where $\psi_a = \int \psi ds$).

Furthermore, $\varphi(s, z) = \psi_\epsilon + s \psi'_\epsilon + s^2 (3\psi_1 - 3\psi_\epsilon - 2\psi'_\epsilon) + s^3 (2\psi_\epsilon + \psi_\epsilon - \psi_1).$

Consequently,

$$\Phi^* \equiv \Phi^*(\theta, z) = \frac{\partial \psi^*}{\partial \theta} = \begin{cases} \frac{\partial \psi}{\partial s} \frac{ds}{d\theta}, & \text{if } s \leq 1 - \epsilon, \\ \frac{\partial \varphi}{\partial s} \frac{ds}{d\theta}, & \text{otherwise.} \end{cases}$$

Clearly, $\frac{\partial \varphi}{\partial s} = (s - 1) B_1,$ where

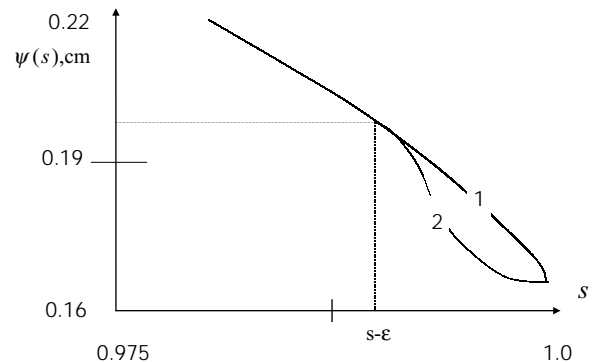


Fig 11. Regularization of the Brooks and Corey model. (1)- $\psi(s) / \psi_a$, (2)- $\psi^*(s) / \psi_a.$

$$B_1 \equiv B_1(s, z) = 6s (\psi_\varepsilon + 0.5\psi'_\varepsilon - \psi_1) - \psi'_\varepsilon.$$

$$\text{Therefore, } \Phi^* = vF, F = \begin{cases} \frac{\Phi}{v}, & \text{if } v > \varepsilon, \\ \tilde{B}_1(v), & \text{otherwise,} \end{cases}$$

$$\text{where, } \tilde{B}_1(v, z) = B_1(s(v), z) s(v) = 1 - \frac{v}{(\theta_{\max} - \theta_{\min})}.$$

The right hand side of Richard's equation becomes

$$\begin{aligned} \frac{\partial}{\partial z} D \frac{\partial \theta}{\partial z} - \frac{\partial K}{\partial z} + T &= - \frac{\partial}{\partial z} D \frac{\partial v}{\partial z} + \frac{\partial}{\partial z} (Fv \frac{d\theta_{\max}}{dz}) - \\ \frac{\partial}{\partial z} (b_1 \mu) + \frac{dK_1}{d\theta_{\max}} \frac{d\theta_{\max}}{dz} + T &= - \frac{\partial}{\partial z} K \Phi^* \frac{\partial v}{\partial z} + \\ \frac{\partial}{\partial z} [v(F \frac{d\theta_{\max}}{dz} - b_1)] + \frac{dK_1}{d\theta_{\max}} \frac{d\theta_{\max}}{dz} + T &= \frac{\partial}{\partial z} K \Phi^* \\ \frac{\partial v}{\partial z} + \frac{\partial}{\partial z} (vb_2) + R + T, b_2 = F \frac{d\theta_{\max}}{dz} - b_1, R &= \frac{dK_1}{d\theta_{\max}} \frac{d\theta_{\max}}{dz}. \end{aligned}$$

Therefore, step 2 is given by

$$\begin{aligned} (\tilde{v}_m^{n+1} - v_m) / \tau &= K_{m+\alpha}^n \Phi_{m+1/2}^n (\tilde{v}_{m+1}^{n+1} - \tilde{v}_m^{n+1}) / \Delta z^2 + \\ (b_2)_{m+1/2} \tilde{v}_{m+\alpha}^{n+1} / \Delta z - K_{m-1+\beta}^n \Phi_{m-1/2}^n (\tilde{v}_m^{n+1} - \tilde{v}_{m-1}^{n+1}) / \Delta z^2 - \\ (b_2)_{m-1/2} \tilde{v}_{m-1+\beta}^{n+1} / \Delta z - R_{m+1}^{n+1} \Omega_m^{n+1} - \hat{T}_m^v, \end{aligned}$$

$$\alpha = \alpha(m) = \begin{cases} 0, & \text{if } (b_2)_m^{n+1/2} \leq 0, \\ 1, & \text{otherwise,} \end{cases} \quad \beta = \beta(m) = \begin{cases} 0, & \text{if } (b_2)_{m-1/2}^n \leq 0, \\ 1, & \text{otherwise.} \end{cases}$$

$$\Omega_m^{n+1} = \begin{cases} (\Omega_1)_m^{n+1}, & \text{if } R_{m+1}^{n+1} > 0, \\ 1, & \text{otherwise,} \end{cases}$$

$$\text{where } \Omega_{1m}^{n+1} = \frac{\tilde{v}_m^{n+1}}{(\Omega_2)_m^{n+1}}, \lim_{n \rightarrow \infty} (\Omega_2)_m^{n+1} \rightarrow \tilde{v}_m^{n+1}, (\Omega_2)_m^{n+1} \rightarrow \tilde{v}_m^n + \varepsilon.$$

Finally, the correction step does not require modifications.

Remark Our numerical experiments reveal that a *substantial* correction is only required if at least one of the auxiliary functions contacts the curve $\chi(z) = \theta_{\max}(z) - \theta_{\min}(z)$ or the line $z=0$. In this case conventional schemes are practically inefficient whereas our method converges to the numerical solution which satisfies the prescribed constraints. However, if $\theta(z, t)$ does not approach the prescribed bounds, the three-step procedure does not have particular advantages. In this case our algorithm generates numerical solutions practically identical to those produced by the conventional schemes.

Theorem 6 *The numerical solution satisfies*

$$(\theta_{\min})_m \leq \theta_m^{n+1} \leq (\theta_{\max})_m.$$

A proof of the theorem can be obtained along the lines of Theorem 4.

Fig 12 shows calculations performed by the proposed method in the case of the infiltration problem. The time and the space step are identical to those employed by the conventional method (Fig 8-9). The solution corresponds to the so-called Hortonian classical mechanism of the runoff production.⁸ When a precipitation rate at the upper boundary exceeds $K(\theta_{\max})$ the moisture profile increases at the soil surface as a function of time. At some point the surface becomes saturated and the inverted zone of saturation begins to propagate downward into the soil.

Clearly, the method establishes the convergence and generates an oscillation-free numerical solution. Fig 13 shows the relationship between $\mu(z, t)$, $v(z, t)$ and $\chi(z)$. The auxiliary variables satisfy $0 \leq \mu(z, t) \leq \chi(z)$, $0 \leq v(z, t) \leq \chi(z)$, $\forall t$.

Table 2 reveals an overall priority of the proposed scheme with regard to conventional methods. S_1 denotes the maximum/average number of iterations

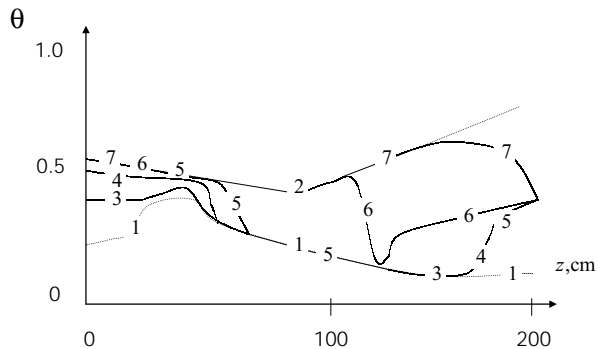


Fig 12. Numerical solution of the infiltration problem, (1) $-\theta_{\min}$, (2) $-\theta_{\max}$, (3) $\theta(z, t)$, $t=0.25h$, (4) $\theta(z, t)$, $t=0.5h$, (5) $t=2h$, (6) $t=4h$, (7) $t=6h$.

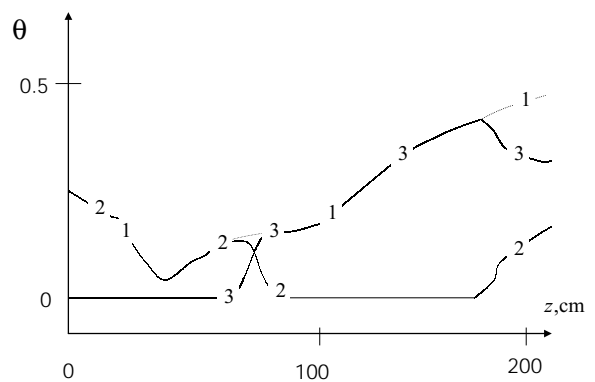


Fig 13. Numerical solution of the infiltration problem, (1) $-\theta_{\max} - \theta_{\min}$, (2) and (3) the auxiliary variables corresponding to step 1 and 2 at $t=2h$. (2) $-m(z, t)$ $\tau=2h$, (3) $v(z, t)$

Table 2. Efficiency of the algorithm. Infiltration problem.

S_1	S_2	$S\tau$	τ , sec	Δ , cm
8/6	4/3(-)	0.11	10	10
8/7	5/4(-)	0.22	10	5
13/9	13/11	0.43	10	2.5
20/12	20/12	0.88	10	1.25
10/9	9/7(-)	0.55	50	10
13/11	Diverges	1.1	50	5
20/13	Diverges	2.15	50	2.5
28/21	Diverges	4.4	50	1.25
22/16	Diverges	11	1000	10
30/21	Diverges	22	1000	5
46/27	Diverges	44	1000	2.5
72/30	Diverges	88	1000	1.25
46/20	Diverges	110	10000	10
65/28	Diverges	220	10000	5
100/46	Diverges	430	10000	2.5
154/65	Diverges	880	10000	1.25

required by the proposed method, S_2 the number of iterations required by the standard symmetric fully implicit, iterative scheme, the symbol (-) indicates violations of the prescribed bounds. $S\tau = \tau / \tau_{CFL}$ where τ_{CFL} is the time step required by the fully explicit, second order scheme, characterized by the CFL-type condition, Note, that although $S\tau < 1$ implies that the explicit scheme converges, it does not necessarily guarantee $(\theta_{min})_m \leq \theta_m^{n+1} \leq (\theta_{max})_m$.

We have performed a large series of numerical experiments to simulate the soil water propagation characterized by randomly perturbed bounds given by

$$\theta_{max}(z) = \bar{\theta}_{max}(z) + \Theta_{max}, \theta_{min}(z) = \bar{\theta}_{min}(z) + \Theta_{min},$$

where $\bar{\theta}_{max}(z), \bar{\theta}_{min}(z)$ correspond to average values of $\theta_{max}(z)$ and $\theta_{min}(z)$, whereas $\Theta_{max}, \Theta_{min}$ are the “high frequency components” generated randomly. Although such examples are not likely to often appear in the practice of conventional soil water modeling, the simulations constitute a very good test of reliability of the numerical schemes.

A typical example(Fig 14) is a “saturation wave” propagating inside the soil.

The wave is modeled by means of the following boundary conditions

$$\theta(0,t) = \begin{cases} \theta_{max}, & 0 \leq t \leq 0.5 \text{ (hour)} \\ 0, & \text{otherwise.} \end{cases} \quad \theta(200,t) = \theta_{max}.$$

The example can be interpreted as a model of the soil saturation induced by a storm following a dry period. The upper zones are quickly saturated or nearly so, establishing two opposite gradients of

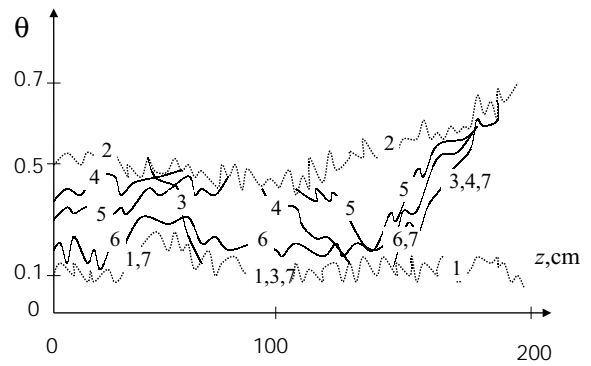


Fig 14. Saturation wave. The numerical solution in the case of randomly perturbed bounds (1)- θ_{min} , (2)- θ_{max} , (3) $\theta(z,t)$, $t=2h$ (3) $t=3h$ (4) $t=4h$ (5) $t=5h$ (6) $t=6h$.

the soil moisture(curve 3 , 4 and 5). The moisture decreases with the depth up to a point when it starts increasing from the previously dry conditions. After the soil water percolates down, the system returns to the initial state.

Table 3 reveals an overall priority of the proposed scheme with regard to the conventional methods. Note, that in this case S_1, S_2 and $S\tau$ represent average values obtained after 100 trials of the random components.

Finally, we analyze the convergence rate. The error is estimated by $\|\theta - \theta_f\|_C, \|\theta - \theta_f\|_{L_1}$ and $\|\theta - \theta_f\|_{L_2}$, where θ_f is the solution obtained by the conventional scheme on a fine grid. The numerical experiments reveal that the convergence rate varies between $\Delta z^{0.9}$ and $\Delta z^{1.35}$ irrespectively of the norm.

Table 3. Efficiency of the algorithm. Saturation wave. Randomly perturbed constraints.

S_1	S_2	$S\tau$	τ , sec	Δ , cm
12/8	3/2(-)	0.05	10	10
18/10	5/3(-)	0.1	10	5
26/12	7/5	0.2	10	2.5
36/20	14/7	0.4	10	1.25
18/10	10/6(-)	0.25	50	10
19/11	Diverges	0.5	50	5
46/14	Diverges	1.1	50	2.5
48/22	Diverges	2.2	50	1.25
30/10	Diverges	4.7	1000	10
44/19	Diverges	8.3	1000	5
64/21	Diverges	16.3	1000	2.5
98/25	Diverges	32.6	1000	1.25
40/14	Diverges	41	10000	10
58/18	Diverges	81	10000	5
90/25	Diverges	163	10000	2.5
138/30	Diverges	326	10000	1.25

CONCLUSIONS

We introduce two new numerical algorithms to treat numerically the Richard's type models of unsaturated porous medium flows. The algorithms generalize our previous results obtained for the diffusion wave equation. The basic properties of the algorithms include convergence and the discrete mass conservation law.

The methodological applications show that when the solution approaches the prescribed boundaries our schemes establish the convergence, stability and produce an oscillation free numerical solution whereas conventional methods are practically inefficient. Moreover, for large time steps, the algorithms (as applied to simulate the unsaturated porous medium flows) provide an overall priority with regard to standard methods in terms of required iterations

Finally, the presented algorithms combined with the preceding results constitute a new family of numerical methods designed to solve the degenerate, non-linear parabolic equations with the constraints imposed a priori on the solution.

REFERENCES

1. MB Abbot & GS Rodenhuis(1982) Numerical modeling of water waves, flows and transport, *Danish Hydr* **15**, 6-23.
2. K Amano(1995) Approximate General Solution of Degenerate Parabolic Equations Related to Population Genetics, *Electronic Journal of Differential Equations* **15**, 1-14.
3. SN Antontsev, GP Epihov GP & AA Kashevarov (1986) Mathematical modeling of water-exchange processes. Novosibirsk, Nauka(in Russian).
4. GI Barenblatt & MI Vishik (1956) On a Finite Velocity in Problems of Nonstationary Filtration of a Liquid and Gas, *Applied Mathematics and Mechanics* **20**(3), 411-7 (in Russian).
5. PD Bates & MG Anderson (1993) A 2D Finite Element Model for River Flow Inundation, *Proc Roy Soc, Ser A*, **400** (1909), 481-91.
6. N Beyer & C Portner (1994) Mike11: Hydrodynamics Simulation of Flood Protection Systems, Proc. 1st Int Conf Hydroinformatics '94, Delft, Netherlands, Sept, 19-23, 407-14.
7. RL Bras(1990), Hydrology, Addison-Wesley.
8. RH Brooks & AT Corey(1966) Properties of Porous Media Affecting Fluid Flow, *J Irrig and Drain, Div ASCE*, **92**, 61-88.
9. B Cappelaere(1997) Accurate Diffusive Wave Routing, *Journal of Hydr Eng, ASCE*, **123**(3), 174-81.
10. VT Chow, DR Maidment & LW Mays (1988) Applied Hydrology. McGraw-Hill.
11. AB Cunningsum & PJ Sinclair (1979) Application and Analysis of Coupled Surface and Groundwater Models. *J Hydr* **43**(1), 129-48.
12. OJ Duru & AT Hjelmfelt (1994) Investigating Prediction Capability of HEC-1 and KINEROS Kinematic Wave Runoff Models. *J Hydr* **157**, 87-103.
13. JR Esteban & JL Vazquez (1986) On the Equation of Turbulent Filtration in One-Dimensional Porous Media, Non-linear Analysis, TMA **10**(11), 1303-25.
14. SO Eching, JW Hopmans & O Wendroth (1994) Unsaturated Hydraulic Conductivity from a Transient Multi Step Outflow and Soil Water Pressure. *Soil Sci Soc Am J* **58**, 687-95.
15. DL Fread (1985) Channel Routing: Hydrological Forecasting. Wiley, New York.
16. RA Freeze (1972) Role of Sub-surface Flow in Generating Surface Runoff. Part 1: Base Flow Contributions to Channel Flow, *Water Resources Research* **8**(3), 609-23.
17. M Th Van Genuchten & DR Nielsen (1985) On Describing and Predicting the Hydraulic Properties of Unsaturated Soils. *Annales, Geophysicae* **3**, 615-28.
18. M Th Van Genuchten (1980) A Closed-form Equation for Predicting the Hydraulic Conductivity of Unsaturated Soils, *Soil Sci, Soc, Am J* **44**, 892-8.
19. RG Hills, I Porro, DB Hudson & PJ Wierenga (1989) Modeling One-dimensional Infiltration into Very Dry Soils 1. Model Development and Evaluation. *Water Resour Res* **25**, 1259-69.
20. WA Jury, WR Gardner & WH Gardner (1991) Soil Physics, John Wiley & Sons.
21. J Kacur, A Handlovicova & M Kacurova (1993) Solution of Non-Linear Diffusion Problems by Linear Approximation Schemes, *SIAM J, Numer Anal* **30** (6), 1703-22.
22. J Kacur (1990) On a Solution of Degenerate Elliptic-Parabolic Systems in Orlicz-Sobolev Spaces I, II, *Math Zeitschrift* **203**, 153-71, 659-79.
23. LS Kuchment, VN Demidov & Yu G Motovilov (1983) Formation of a River Discharge. Moscow, Nauka.
24. LS Kuchment & AN Gelfan (1993) Dynamic-stochastic Models of River Flows. Moscow, Nauka.
25. JJ Leenderse & EC Criton (1971) A Water Quality Simulation Model for Well-mixed Estuaries and Coastal Seas, Vols. I and II. The Rand Corporation, Technical Report R- 709.
26. SS Makhanov & A Yu Semenov (1994) A Stable Non-negative Numerical Method for Calculating the Flow of a Liquid in the Open Channel. *Comp Maths and Math Phys Elsevier* **34** (1), 104-17.
27. SS Makhanov & A Yu Semenov (1996) A Two Dimensional Non-Negative Algorithm for Calculating the Flow of a Liquid in an Open Channel, *J Comp Maths Math Phys Elsevier* **4**, 501-7.
28. SS Makhanov (1999) Flood Modeling in East Bangkok, *Proc Civil and Environ Eng Conf, New Frontiers and Challenges, 8-12 November, 1999, Bangkok*, 5 (Part I), 111-120.
29. SS Makhanov (2000) Numerical Schemes for Non-linear Parabolic Equations with A Priori Bounded Solution, *Proc IMACS Word Congress on Computational Mathematics and Simulations, Switzerland 21-25 August, 23-29, 2000*.
30. SS Makhanov, S Vannakrairojn & EJ Vanderperre (1999) A Two-Dimensional Numerical Model of Flooding in East-Bangkok, *Journal of Hydr Eng ASCE*, **25** (4) 407-416.
31. SS Makhanov, EJ Vanderperre & K Sonthipaumpoon (1999) On Generation of Curvilinear Grids, *South-East Asian Bulletin of Mathematics*, Springer Verlag **23**, 231-41.
32. A Martinez, A Marquina & R Donat (1994) Shooting Methods for 1D Diffusion-Absorption Problems. *SIAM J Numer Anal*, **31**(2), 572-89.
33. MG McDonald & AW Harbangh (1988) A Modular Three-dimensional Finite-Difference Groundwater Flow Model. *US Geolog Survey Open-File Rep N83-875*, Washington
34. Master Plan Study on the Water Management System and Monitoring Program in the Chao-Phraya River Basin (1989) Final Report, Ministry of Agriculture and Cooperatives, Royal Irrigation Department, Thailand.
35. ID Moore & RB Crayson (1991) Terrain-based Catchment Partitioning and Runoff Prediction Using Vector Elevation Data. *Water Resources Research* **27**, pp 1177-91.

36. AZE Rasul & MF Rabbi (1994) GIS in Flood Mapping for Improved Flood Management in Bangladesh *Proc the 1st Int Conf Hydroinformatics'94, Delft, Netherlands, 19-23 Sept, 1994*, 629-34.
37. AA Samarski (1988) Numerical Methods. Moscow, Nauka (in Russian).
38. VP Singh & M Prasana (1999) Generalized Flux Law, with Application, *Hydr Processes* **13**, 73-87.
39. WJ Syme & GN Paudyal (1994) Bangladesh Flood Management Model. *Proc 2nd Int Conf on River Flood Hydraulics, 22-25 March, York, England*, 167-76.
40. T Takasao & M Shiiba (1988) Incorporation of the Effect of Concentration of Flow into the Kinematic Wave Equations and its Application to Runoff System Lumping, *J Hydr* **102**, 301-22.
41. T Tingsanchai & NK Lal (1988) Subsidence of Flood Waves in Overbank Flow Areas. *J of Hydrol Res* **26** (5), 585-97.
42. AF Voevodin & SF Shugrin (1981) Numerical Methods for Calculations of 1D Systems. Novosibirsk, Nauka.
43. NE Voltsinger & RV Pyaskovsky (1977) Shallow Water Theory. Oceanological Problems and Numerical Methods, Leningrad, Gidrometeoizdat (in Russian).
44. W Wu & RC Sidle (1995) A Distributed Slope Stability Model for Steep Forested Basins. *Water Resources Research* **31** (8), 2097-110.